

Effects of social presence on behavioural, neural and physiological aspects of empathy for pain

Abbreviated title: Effects of social presence on empathy for pain

Pauline Petereit^{1,2*}, Ronja Weiblen^{1,2,3}, Anat Perry⁴, Ulrike M. Krämer^{1,2,5*}

¹ Department of Neurology, University of Lübeck, 23562 Lübeck, Germany

² Center of Brain, Behavior and Metabolism (CBBM), University of Lübeck, 23562 Lübeck, Germany

³ Department of Psychiatry and Psychotherapy, University of Lübeck, 23562 Lübeck, Germany

⁴ Psychology Department, Hebrew University of Jerusalem, Jerusalem, Israel

⁵ Department of Psychology, University of Lübeck, 23562 Lübeck, Germany

* Corresponding authors: Pauline Petereit, pauline.petereit@neuro.uni-luebeck.de; Ulrike M. Krämer, ulrike.kraemer@uni-luebeck.de

Number of pages: 34

Number of figures: 5

Number of tables: 1

Number of words in abstract: 241

Number of words in introduction: 643

Number of words in discussion: 1482

Conflict of interest statement: "The authors declare no competing financial interests."

Acknowledgements:

UMK is supported by the German Science Foundation (grant number KR3691/8-1). We thank Lou Maria Lütjohann, Celina Mävers, Marthe Mieling, Leah Reinicke, Elynn Sängner and Jasmin Thurley for help with data collection and pre-processing, and Charlotte Petereit for help with the figures.

31
32
33
34
35
36
37
38
39
40
41
42
43
44
45
46
47
48
49
50
51
52
53
54
55
56
57
58
59
60
61
62

Abstract

Social interactions are rich in cues about others' mental and emotional states, and these cues have been shown to facilitate empathy. As more and more social interactions shift from direct to mediated interactions with reduced social cues, it's possible that empathy is affected. We tested whether behavioural, neural and physiological aspects of empathy for pain are reduced in a video-mediated interaction. To this end, 30 human participants (23 females, 7 males) observed one of 5 targets (all female) undergoing painful electric stimulation, once in a direct interaction and once in a live, video-mediated interaction (within-subject design) while EEG was measured. On a behavioural level, we found that observers were as accurate in judging others' pain via video as in a direct encounter and reported the same level of distress. On the neural and physiological levels, the theta response to others' pain and skin conductance coupling in the dyad were reduced in the mediated condition. Other measures, including mu suppression (a common marker of pain empathy), were not affected by condition. To conclude, a video-mediated interaction did not impair the cognitive aspects of empathy for pain, i.e., understanding the other accurately. However, the reduced theta response and reduced skin conductance coupling suggest that physical proximity with its rich social cues is important for other stimulus-driven physiological responses that may be related to resonance with the other's experience. Our results encourage more research on the role of social presence for different empathy components.

Key words: social presence, pain empathy, empathic accuracy, mu suppression, physiological coupling

Significance Statement

In mediated interactions (e.g. video calls), less information is available about the other. However, no study so far has investigated how this affects our empathy for one another. Here we show in human dyads that while some cognitive and affective aspects of pain empathy are unchanged in a video-mediated compared to direct interaction, some neural and physiological aspects of pain empathy are reduced. These results imply that there are neurocognitive consequences to remote social interactions, warranting future studies to confirm these results and to understand their behavioural significance.

63 **Introduction**

64 Over the last decades, many social interactions in private life and at work, including medical and
65 psychotherapeutic contexts, have shifted from personal encounters to mediated interactions such as
66 video calls. These mediums provide less detailed social cues and information channels and limit
67 opportunities for immediate, reciprocal interaction compared to personal interactions. These factors are
68 sometimes referred to as intimacy and immediacy, and together they contribute to the degree of social
69 presence offered within social interactions (Cui et al., 2013; Short et al., 1976; see Biocca et al., 2003,
70 for alternative accounts of social presence). Given the reduced social presence of mediated
71 interactions, the question arises of how this changes our ability to share and understand others' affective
72 states, i.e., our ability to empathize (Decety & Jackson, 2004; Shamay-Tsoory, 2011). Focusing on
73 intimacy, we asked how the reduction of social cues – using a video call versus a direct interaction –
74 affects empathy. We used empathy for pain as a well-established model to investigate the behavioural,
75 neural and physiological aspects of empathy (Singer & Lamm, 2009).

76 Empathy for pain is a multifaceted process, including an affective response, feelings of distress
77 and empathic care towards the person suffering (Goubert et al., 2009; Lamm et al., 2007; Singer &
78 Lamm, 2009), as well as cognitive processes. The latter are sometimes measured as empathic
79 accuracy, which is the accuracy of one's perception of the other's pain (Laursen et al., 2014; Zaki et al.,
80 2009b).

81 On the neural level, empathy for pain has been associated with mu suppression in the EEG:
82 reduced power between 8 and 13 Hz over the somatosensory cortex (Cheng et al., 2008; Gallo et al.,
83 2018; Peled-Avron et al., 2018; Peng et al., 2021; Perry et al., 2010a). Mu suppression has been linked
84 to higher empathic accuracy (Goldstein et al., 2018) and might aid empathy by representing the other's
85 bodily state in one's own somatosensory system (Riečanský & Lamm, 2019). Other studies examined
86 mid-frontal theta activity (4–8 Hz) as a possible electrophysiological component of empathy (Mu et al.,
87 2008; Peng et al., 2021) and own pain experience (Misra et al., 2017; Peng et al., 2021; Ploner et al.,
88 2017). Mid-frontal theta is thought to indicate activity in the anterior cingulate cortex (ACC, Mitchell et
89 al., 2008; van der Molen et al., 2017), which is often reported in fMRI studies on empathy for pain and
90 is associated with the negative affect during own and others' pain (Fallon et al., 2020).

91 Finally, several studies suggest that physiological “coupling” (in cardiac activity or skin
92 conductance), i.e., aligning to the physiological state of someone in pain, might reflect empathic sharing

93 and facilitate understanding of the other (Goldstein et al., 2017; Jospe et al., 2020; Reddan et al., 2020;
94 Zerwas et al., 2021).

95 Humans respond to social cues such as facial expressions or eye contact by sharing the other's
96 emotional state (Ensenberg et al., 2017; Hess, 2021; Perry et al., 2010b). Reducing the availability of
97 social cues and thereby the intimacy of the interaction may thus reduce affective resonance and impair
98 understanding of others. To test the effect of intimacy on empathy for pain in the current study, pairs of
99 participants underwent an empathy-for-pain paradigm in two conditions: one direct, face-to-face
100 interaction and one interaction mediated via real-time video transfer. In both conditions, one participant
101 (the target) received painful electrical stimulation while the other (the observer) was watching. We
102 measured EEG from the observer and behavioural, cardiac and skin conductance responses from both
103 members of the dyad. We hypothesized that the reduced level of intimacy in mediated compared to
104 direct interactions diminishes empathic accuracy (Agahi & Wanic, 2020; Jospe et al., 2020; Zaki et al.,
105 2009a) and affective empathy (Bogdanova et al., 2022; Ionta et al., 2020). We also expected it to reduce
106 neural and physiological responses to another's pain and physiological coupling within the dyad (Murata
107 et al., 2020).

108

109 **Methods**

110 **Participants**

111 Five female psychology students were recruited as targets. Only females were recruited for the targets
112 to reduce possible gender effects over the dyads. They were on average 19.8 years old (SD = 0.75).
113 Thirty psychology students (7 males, 23 females, mean age(SD) = 24.07(4.68) years) were recruited
114 as observers. A priori power analyses with data simulations using the *simr* package (Green & MacLeod,
115 2016) in R showed that this sample size is sufficient to detect a small effect ($f_2 = 0.02$) of condition on
116 empathic accuracy (measured via an interaction effect between shock intensity and direct vs. mediated
117 condition; see below for statistical analyses) with a power of at least 0.98 (depending on exact model
118 structure). For both targets and observers, exclusion criteria were current psychiatric or cardiovascular
119 and past or current neurological disorders, current or chronic pain conditions or current pain-medication
120 intake. For one observer, all physiological data from the own-pain condition had to be excluded because
121 of missing stimulus triggers. Skin conductance and electrocardiogram (ECG) data from one target
122 (mediated-interaction condition) were missing due to a technical error. Skin conductance data from two

123 observers could not be analysed due to poor data quality. These dyads were excluded from all analyses
124 of the missing outcome variable. Targets received €10 per hour; observers received course credit or
125 €10 per hour. All participants provided written informed consent prior to taking part in the study,
126 including consent for video-recording them and showing the videos to other work group members, and
127 in case of the targets, showing the videos to other participants in future studies. The experiment was
128 carried out according to the Declaration of Helsinki and was approved by the Ethics Committee of the
129 University of Lübeck.

130

131 **Experimental design**

132 Each target interacted with six different observers on six different study days. Observers came to the
133 lab once for one session (two interactions) with one target. For the observers, there were three
134 conditions (within-subject design, see Fig. 1A). In the “own pain” condition, the observer was alone in
135 the laboratory and received electric shocks. This ensured that observers knew what the electric shocks
136 felt like. In the “direct interaction” condition, observer and target sat opposite each other at a table, and
137 the target received electric shocks while the observer watched. In the “mediated interaction” condition,
138 target and observer sat in adjacent rooms and saw each other over a real-time video transmission.
139 Observers watched the same target in the latter two conditions and rated the observed pain experience
140 of the target. Targets rated their own pain experience. In all conditions, skin conductance and ECG
141 were recorded from both participants, and EEG was recorded from the observer. The “own pain”
142 condition was always carried out first, and the order of “direct interaction” and “mediated interaction”
143 conditions was pseudo-randomized over participants. In the latter two conditions, targets’ and
144 observers’ behaviour was video-recorded.

145

146 **Stimulus calibration**

147 Prior to the pain task, pain stimuli were calibrated to the subjective pain thresholds of the participants
148 (the observers in the “own pain” condition, and the targets prior to the first interaction condition). To this
149 end, participants received electric shocks starting from 0 mA, increasing in amplitude in steps of 0.5
150 mA. They were required to rate each stimulus on a scale from 0 (“not perceivable”) to 8 (“strongest pain
151 imaginable”). As soon as they rated a stimulus with “7” (“unbearably painful”), stimuli were decreased
152 in amplitude (again in steps of 0.5 mA) until participants rated the stimulus as “0” or an amplitude of 0

153 mA was reached. The procedure was then repeated once more with increasing stimulus intensity. The
154 stimulus intensity that was rated as 1 (“noticeable”) in this last round was used as the lower limit for the
155 stimuli presented during the task, with the stimulus intensity rated as 6 (“extremely painful”) used as the
156 upper limit.

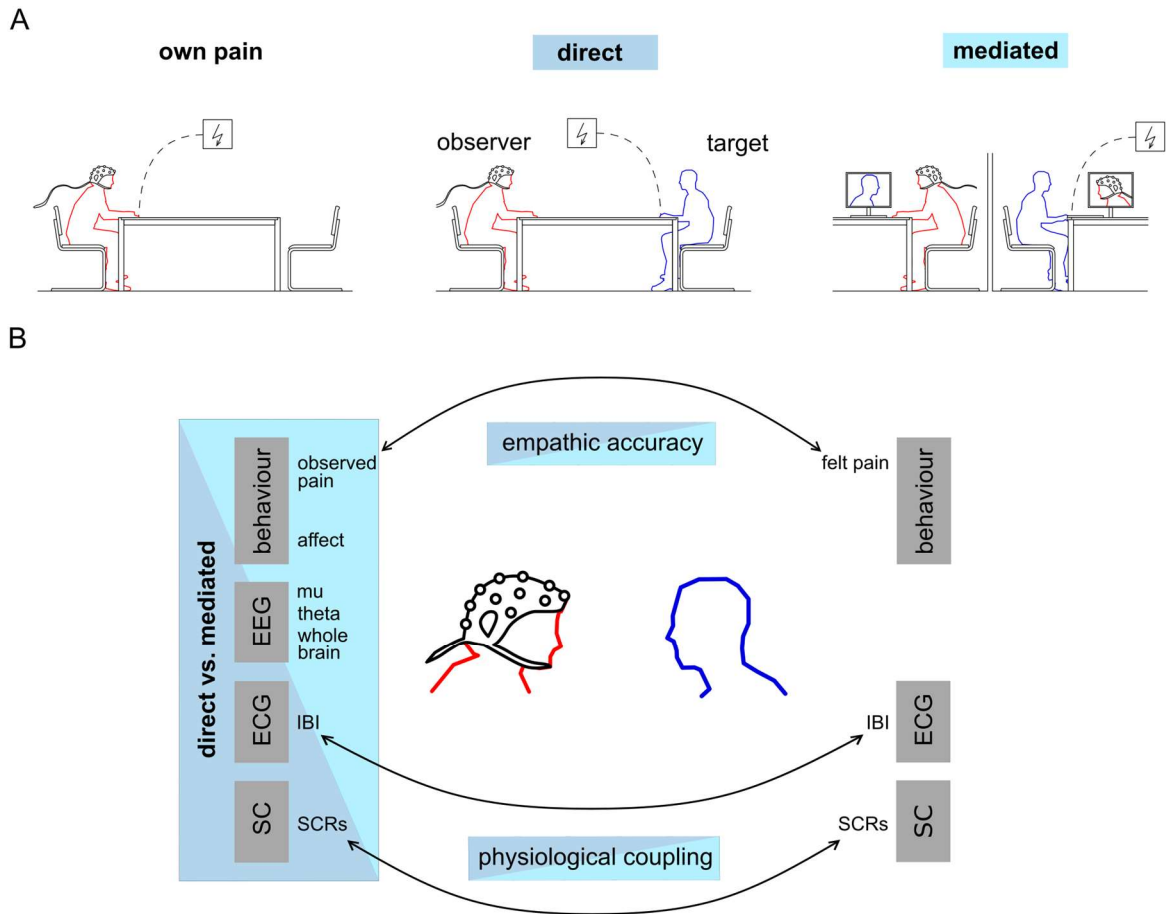
157

158 **Pain task**

159 The pain task itself was adapted from Rutgen and colleagues (2015). Electric shocks were delivered
160 using a DS 5 isolated bipolar constant current stimulator (Digitimer) and a bar electrode (Digitimer, two
161 electrodes with 9-mm diameter, 30 mm apart) attached to the back of the right hand. The skin under
162 the electrode was treated with an abrasive paste and conductive gel to reduce the electric resistance
163 of the skin.

164 Each trial started with an auditory cue lasting 500 ms that did not predict the shock stimulus
165 intensity. At 1000 ms after the cue, the electric shock was delivered for 500 ms (series of 2-ms electric
166 pulses, interspersed with approximately 20-ms breaks). After a randomly varying interval (6000–9000
167 ms), the next trial or the rating followed. In 50% of the trials, participants were prompted to rate the
168 stimulus by a vocal recording saying, “Please rate”. We included the rating only in 50% of the trials to
169 keep the duration of the experiment feasible. The rating was given on a tablet computer. Targets rated
170 how painful the electric shock was for themselves on a visual analogue scale ranging from “not at all
171 painful” to “extremely painful”. Observers rated how painful they thought the electric shock was for the
172 target (on the same visual analogue scale) as well as how unpleasant it was for them to watch the
173 target receive the electric shock (on a visual analogue scale ranging from “not at all unpleasant” to
174 “extremely unpleasant”). The latter rating served as a measure of affective empathy. Electric shocks
175 varied in intensity in 20 steps from the intensity the targets had rated as “noticeable” (intensity level 1)
176 to the intensity they had rated as “extremely painful” (intensity level 20) during the calibration. There
177 were 80 trials in each condition, and each intensity occurred four times. The order of intensities was
178 pseudo-random (with no more than four shocks with intensity level higher than 10 or lower than 11 in a
179 row) but fixed for all participants and conditions. The order of trials that had to be rated was fixed as
180 well. In the “own pain” condition, the task was the same except that observers rated their own pain
181 experience on the visual analogue scale. Targets and observers were instructed not to talk or move

182 excessively during the task but were otherwise allowed to express their emotions freely. Observers
183 were instructed to rate the pain of the other as accurately as possible.
184



185
186 **Figure 1.** (A) Schematic overview of experimental conditions. (B) Overview of the analysed outcomes.
187

188 **Experimental procedure**

189 *Target selection*

190 Before targets interacted with observers, they came to the laboratory alone to familiarize themselves
191 with the procedures and the stimuli. In this first session, they did the same pain task as in the main
192 experiment, but with no other person in the room. As in the main experiment, skin conductance and
193 ECG were recorded. After the first session, targets decided whether they wanted to participate in the
194 main experiment. Moreover, we used this first session for target selection, as we aimed to recruit only
195 targets who set the intensity limits of the stimuli during stimulus calibration to a level that was actually
196 painful. This was important to ensure that we measured actual pain empathy during the main
197 experiment. We therefore defined the minimum upper intensity limit that targets had to reach during the

198 first session to be eligible for the full experiment as within +/-1 standard deviation of the mean upper
199 intensity limit of a pilot study (resulting in a minimum upper intensity limit of 2.5 mA). We invited seven
200 potential targets to this first session. Due to the criteria, we had to exclude one target, and one
201 participant dropped out after the first session, which left five targets for the main experiment.

202

203 *Main experiment*

204 For the main experiment, the observer arrived first in the laboratory. After the informed-consent form
205 was signed, the EEG, skin conductance and ECG measurement equipment as well as the stimulus
206 electrode were prepared. The pain-calibration procedure was carried out. After five practice trials to
207 familiarize themselves with the ratings on the tablet computer, participants did the pain task in the “own
208 pain” condition. Meanwhile, the target arrived in a different room, responded to questionnaires and was
209 equipped with the electrodes for physiological measurement. As soon as the “own pain” condition was
210 finished, the stimulus electrode was attached to the target’s right hand, and the target underwent the
211 pain-calibration procedure. Meanwhile, the observer completed questionnaires. When both were
212 finished, the experimental tasks started (see “pain task” above; either “direct interaction” or “mediated
213 interaction” first). Afterwards, target and observer were seated in different rooms again and replied to
214 post-experimental questionnaires. Finally, observers were debriefed about the aim of the study. Targets
215 were debriefed only after completing all six sessions.

216

217 **Questionnaires**

218 We assessed participants’ age, gender, body weight and height, educational degree, and habits
219 regarding smoking, caffeine consumption and physical activity. After the experiment, we obtained
220 participants’ subjective evaluation of the experiment and observers’ evaluation of the target. They also
221 filled out two personality questionnaires: the Interpersonal Reactivity Index (Davis, 1983; German
222 version: Paulus, 2009) and the Emotion Regulation Questionnaire (Gross & John, 2003; German
223 version: Abler & Kessler, 2009). These data are not further evaluated here.

224

225 **Physiological data acquisition**

226 Participants were asked to refrain from smoking, exercise, alcohol and caffeine for at least six hours
227 before the experiment to prevent these factors from impacting the physiological measurements. EEG

228 data were recorded with 59 Ag/AgCl electrodes placed on an elastic cap according to the international
229 10-20-system (using a BrainAmp MR plus amplifier, BrainProducts GmbH). An online reference
230 electrode was placed on the left earlobe, while an offline reference electrode was placed on the right
231 earlobe. Horizontal and vertical EOG were recorded with four electrodes placed next to the outer
232 corners of the eyes and above and below the left eye, respectively. Sampling rate was 500 Hz, and
233 data were recorded with an online high pass filter of 0.016 Hz, a low pass filter of 48 Hz and a notch
234 filter at 50 Hz. Impedances were kept below 5k Ω .

235 ECG data were recorded with bipolar Ag/AgCl recording electrodes and one reference
236 electrode, using a 50-Hz notch filter. One of the recording electrodes was placed on the right forearm,
237 the other one on the left lower calf of the participant (following Einthoven lead II configuration, Einthoven
238 et al., 1950). Skin conductance was measured with two electrodes placed on the thenar and hypothenar
239 of the left hand, using a 50-Hz notch filter. An electrode attached to the left forearm served as ground
240 for both ECG and skin conductance, which were recorded with the same amplifier (BrainAmp ExG,
241 BrainProducts GmbH). In the “direct interaction” and “mediated interaction” conditions, data from
242 observer and target were recorded synchronously by connecting all amplifiers to the same USB adapter
243 feeding the data into BrainVisionRecorder (version 1.21.0102, BrainProducts GmbH).

244

245 **Physiological data processing**

246 *EEG data*

247 All pre-processing was done in EEGLAB, version 2020.0 (Delorme & Makeig, 2004), implemented in
248 MATLAB R2019b (The Mathworks). Data were re-referenced to the right earlobe, and bipolar horizontal
249 and vertical EOG channels were computed. Consistently bad channels (mean number = 2.01, range =
250 0 to 8 channels per participant and condition) and data segments with large artefacts were removed
251 from the data (resulting in on average 1.6% of removed trials per participant and condition in the final
252 epoched data). A bandpass filter was applied (finite impulse response filter, lower limit: 1 Hz, upper
253 limit: 40 Hz, filterorder: 16500). Next, independent component analysis (ICA; implemented with the
254 *runica* function in EEGLAB) was used for ocular artefact correction. Independent components that were
255 clearly related to eye blinks or horizontal eye movements based on topography and time course were
256 visually detected and removed (ranging from 2 to 6 components per participant). Afterwards, the
257 weights of the remaining components were projected onto the original unfiltered data (Stropahl et al.,

258 2018). Channels that had been removed before the ICA were interpolated (spherical interpolation); For
259 some participants additional bad channels (mean number = 0.44, range = 0 to 3 channels per participant
260 and condition) had to be interpolated. Data were then filtered with a bandpass filter with a lower limit of
261 0.2 Hz and an upper limit of 40 Hz (Finite impulse response filter, filter order = 16500, hamming window).
262 Afterwards, data were segmented into stimulus-locked epochs of 4500-ms lengths (1000 ms before
263 and 3500 ms after stimulus onset) and baseline-corrected to 1000 ms before stimulus onset. A voltage
264 threshold (between -70/70 μV and -100/100 μV) was manually set for each participant in a way that all
265 trials with non-ocular artefacts were removed. The number of rejected trials varied from 0 to 31% per
266 participant and condition and did not differ between conditions ($M = 13\%$ in all conditions).

267 For the time-frequency analysis, single-trial data of all electrodes were convolved with a
268 complex Morlet wavelet as implemented in MATLAB (function *cwt* with parameter specification 'cmor1-
269 1.5'):

$$270 \quad \omega(t) = (\pi f_b)^{-0.5} e^{-2\pi i f_c t} e^{-\frac{t^2}{T_b}},$$

271 where $f_b = 1$ is the bandwidth parameter, and $f_c = 1.5$ is the wavelet center frequency. Specifically, for
272 each participant, changes in time-varying energy were computed (square of the convolution between
273 wavelet and signal) in the frequencies (1–40 Hz, linear increase) for the 1500 ms after shock onset.
274 Power values were converted to decibels with respect to an average baseline from 500 to 50 ms before
275 stimulus onset (Cohen, 2014). For analyses of peak-frequency power (see next paragraph), we
276 subtracted the averaged data from 500 to 50 ms before stimulus onset as a baseline correction.

277 To analyse mu suppression, we determined the individual peak frequency of mu power for each
278 participant by using the *restingIAF* toolbox (Corcoran et al., 2018). Frequency peaks in the range from
279 8 to 13 Hz were detected in the baseline data from 1000 to 0 ms before shock onset in the “own pain”
280 condition at central electrodes (C1, C2, C3, C4, C5, C6, CP1, CP2, CP3, CP4, CP5, CP6, FC1, FC2,
281 FC3, FC4, FC5, FC6). For each detected frequency peak, the difference in average power between
282 baseline (-1000 to 0 ms) and stimulation (0 to 1000 ms after shock onset) was calculated. The electrode
283 and corresponding peak frequency with the strongest shock-related desynchronization for each
284 participant was chosen for all further analyses. In 16 participants, a clear peak frequency was
285 detectable. Peaks occurred at all possible frequencies except 9 Hz, and at the following electrodes: C1,
286 C4, C3, CP2, CP3, C6, CP6, FC6, and FC2. The remaining 13 participants did not show a peak

287 frequency, and for them data from the most frequent peak frequency and electrode were used (11 Hz
288 at C4).

289

290 *ECG data*

291 ECG data were loaded into EEGLAB, filtered with a bandpass filter (lower: 1 Hz, upper: 30 Hz, finite
292 impulse response filter, filterorder = 8250) and segmented into epochs of 2 s before and 8 s after
293 stimulus onset for the stimulus-locked analyses. The MATLAB function *findpeaks* was used to detect
294 the r-peaks in the segmented as well as the continuous data (for additional analyses of physiological
295 coupling). Afterwards, data were visually screened for wrongly assigned or missing r-peaks. Data
296 sections containing extrasystoles or otherwise undetectable R-peaks were treated as missing values.
297 The interbeat interval (IBI) in ms was calculated for every pair of heartbeats and used as IBI value for
298 each original data point in between the two heartbeats. In this way, the IBI trace had the same time
299 resolution as the original data. For the analysis of condition differences in IBI responses to shocks, the
300 mean IBI from 2 to 5 s after cue onset (Sperl et al., 2016) was computed and baseline-corrected to the
301 mean of the 2 s before cue onset.

302

303 *Skin conductance data*

304 Skin conductance responses (SCRs) were analysed using the Ledalab-Toolbox (Benedek &
305 Kaernbach, 2010, version 3.4.8) in Matlab. Data were downsampled to 50 Hz, smoothed and visually
306 screened for strong artefacts, which were spline-interpolated. Afterwards, a continuous deconvolution
307 analysis was conducted to separate phasic from tonic skin conductance activity (Benedek & Kaernbach,
308 2010). In the following, the mean phasic driver activity 1–4 s after shock onset was used for analyses
309 (for targets' SCR in physiological coupling). For the observer data (condition differences and
310 physiological coupling), four different time lags (1–4 s) were considered to account for a time lag in the
311 observer's response to the target's pain expression.

312

313 **Statistical analyses**

314 We first outline the general statistical analysis approach before specifying the details. One set of
315 statistical analyses examined the observers' responses to the targets' pain (empathic accuracy,
316 unpleasantness ratings, neural and physiological responses; see Fig. 1B, left side). In these analyses,

317 the predictors, shock intensity, condition (direct vs. mediated) and their interaction were tested. A
318 significant effect of shock intensity indicates that the observer's responses are influenced by the other's
319 pain and are therefore interpreted as empathic. A significant effect of condition indicates that social
320 presence generally changes the observers' behaviour and physiology, whereas an interaction between
321 shock intensity and condition indicates that social presence alters the sensitivity to another's pain. The
322 second set of analyses examined physiological coupling between observer and target responses (see
323 Fig. 1B, bottom). In these analyses, the targets' responses, the condition (direct vs. mediated) and their
324 interaction served as predictors. A significant effect of targets' responses indicates that observers' and
325 targets' responses are generally coupled, whereas an interaction with condition indicates stronger
326 coupling in one condition compared to the other.

327 In both sets of analyses, (generalized) linear mixed models with single trials (Level 1) nested
328 in observers (Level 2) and observers nested in targets (Level 3) were calculated. For theta activity,
329 responses were averaged over trials. For the peak-mu analysis, permutation tests over the whole time
330 course were conducted, as there was no predefined time window. To test for effects of intensity,
331 condition and their interaction beyond mu suppression, exploratory permutation tests on the whole EEG
332 data space were conducted.

333 To assess the robustness of the findings, the analyses of mu, IBI and SCRs were repeated with
334 data averaged over trials. In these analyses, the factor intensity was dichotomized into low and high
335 intensity (low: 1 to 10; high: 11 to 20). The results of these analyses are not reported, as they did not
336 differ from the single-trial results. In the figures, data are dichotomized into low and high intensities for
337 display purposes only. Permutation tests were carried out in MATLAB (version R2019b, The
338 Mathworks), and all other statistical analyses were carried out in R (version 4.0.2, *R core team*).

339

340 *Behavioural data*

341 To test for condition differences in empathic accuracy, we conducted a negative binomial generalized
342 linear mixed model (using the function *glmer.nb* in the *lme4* package in R, Bates et al., 2020) on
343 observers' single-trial ratings of the other's pain (Lawless, 1987). To find the best random slopes
344 structure, first models with the full fixed-effects structure and different random slopes were compared
345 using the Akaike Information Criterion (AIC, Akaike, 1998). An AIC difference greater than 2 was set as
346 the threshold for a significant difference (Burnham & Anderson, 2004). Then one fixed predictor after

347 the other was added to the model with the optimized random-effects structure, and only predictors that
348 significantly improved the model were kept. The same procedure was used to test for differences in
349 unpleasantness ratings between the conditions.

350

351 *EEG data*

352 To test whether mu suppression was modulated by shock intensity (20 levels), condition (direct vs.
353 mediated) or their interaction, permutation tests were conducted on the mu peak-frequency power
354 within the window from -500 to 1500 ms after stimulus onset (see Cohen, 2014). To test for effects of
355 shock intensity on mu suppression, Spearman correlations between normalized single-trial power and
356 single-trial shock intensity were calculated for each data point and across participants. This yielded a
357 time course of correlation coefficients between peak-frequency power and shock intensity. Correlation
358 values were z-transformed by comparing them to a permutation-based null-hypothesis distribution
359 (based on randomly shuffling over trials 1000 times). To correct for multiple comparisons, a maximum
360 value correction was used (Cohen, 2014).

361 To test for condition differences in mu suppression regardless of shock intensity, mu power
362 was averaged over trials and compared between conditions. For the null-hypothesis distribution, the
363 assignment of condition was randomly shuffled over participants (1000 permutations). To test for
364 condition differences in the correlation between shock intensity and power (whether power tracked
365 shock intensity to a larger degree in the direct condition), the condition difference between correlation
366 coefficients was calculated for each data point and participant and compared to a random distribution
367 (shuffled between conditions in 1000 permutations). For a comparison, we also analysed power in the
368 traditional mu band (8–13 Hz, electrode C4, 500–1000 ms after shock onset). We chose the time
369 window according to previous literature and to be comparable to the time window in which the response
370 to own pain occurred (Zebarjadi et al., 2021).

371 For the effects of condition, shock intensity and their interaction on theta responses, we
372 analysed power in the traditional theta band (4–8 Hz, electrode Fz, 0–500 ms after shock onset). We
373 chose the time window according to previous literature (Mu et al., 2008; Peng et al., 2021). In the latter
374 two analyses, we used a linear mixed model with condition averages nested in observers and observers
375 nested in targets and dichotomized shock intensities.

376 Finally, in an exploratory analysis, using the same permutation test method as described above
377 for peak-frequency μ , we looked for main effects of shock intensity (20 levels), condition and their
378 interaction on power across the whole time-frequency-electrode space (1–20 Hz, all electrodes). For
379 the effect of shock intensity, a time window from 0 to 1500 ms was used, for the other analyses a time
380 window from -500 to 1500 ms. For the effect of shock intensity data were downsampled to 125 Hz to
381 reduce computation time. Again, a maximum value correction and additionally a cluster size correction
382 (Cohen, 2014) were used to correct for multiple comparisons.

383

384 *IBI and SCRs*

385 To test for condition and shock intensity (20 levels) effects on the observers' IBI, linear mixed models
386 on the single-trial IBI averages were conducted (using the *lmer* function in *lme4* in R). The same
387 procedure was used for the skin conductance data. Here, first the time lag with the greatest SCR over
388 all conditions was selected for further analyses. To account for interindividual variation in SCR levels,
389 SCR means were normalized by dividing them by participants' individual standard deviation. As SCR
390 data were not normally distributed, generalized linear mixed models (using the *glmer* function in *lme4*,
391 Gamma family, log-link function) were used for these data. To assess the robustness of the findings,
392 all analyses were also carried out with data averaged over trials (with dichotomized shock intensities).

393 To test for coupling between targets' and observers' IBI and SCRs, similar (generalized) linear
394 mixed models were used, but this time the targets' IBI response or SCR was entered as a fixed predictor
395 instead of the stimulus intensity. For all (generalized) linear mixed models, fitting of random- and fixed-
396 effects structure was carried out in the same way as for the single-trial behavioural data. To assess the
397 robustness of the findings, skin conductance coupling was also analysed by calculating Spearman's
398 correlation coefficients between targets' and observers' SCRs and comparing them between conditions
399 using a linear mixed model. Correlations were calculated for the four time lags, and the time lag with
400 the highest correlation coefficients across both conditions was chosen for the linear mixed model. For
401 the robustness analysis of the IBI coupling, the Spearman's correlation between the targets' and the
402 observers' continuous IBI over the whole task was calculated. For this, IBI data were smoothed with a
403 moving average function of 2 seconds to reduce the influence of strong outliers. The correlation
404 coefficients were calculated for 20 different time lags (steps of 0.5 s) between target and observer data.
405 For testing condition effects, the lag with the highest correlation over all conditions was used.

406 Correlation coefficients were transformed using the Fisher's z-transformation to obtain normally
407 distributed data. They were then compared between conditions using linear mixed models with
408 correlation coefficients from different conditions (Level 1) nested in observers (Level 2) and targets
409 (Level 3). The results of these analyses are reported in the results section when they diverge from the
410 results of the single-trial analyses.

411

412 **Control analysis of target expressivity**

413 Empathic accuracy depends on the expressivity of the other (Zaki et al., 2008), and differences between
414 direct and mediated interactions might result from altered expressivity of the targets in either condition.
415 To test whether the targets show systematic differences in their pain expression between the conditions,
416 a control experiment with a different sample was conducted. Thirty-one participants (25 females, 6
417 males, mean age(SD) = 23.51(4.70)) were shown 100 segments from the video recordings of both
418 direct and mediated interaction without being aware of that manipulation. Video segments included four
419 seconds before and four seconds after an electric shock and were chosen such that there was an equal
420 number of videos from each original session, condition and target pain rating (summarized in 5 bins of
421 20 rating points each). Videos were shown in random order. After each video the participants had 10
422 seconds to rate how painful the stimulus was for the target in the video on a visual analogue scale
423 ranging from "not painful at all" to "extremely painful". If targets expressed their pain differently in the
424 two conditions, we would expect condition differences in the mean pain ratings or in the empathic
425 accuracy of the control participants. Mean pain ratings and mean empathic accuracy scores
426 (Spearman's correlations) were then compared between the conditions using t-tests.

427

428 **Pre-registration and data availability**

429 A pilot study using a similar design was pre-registered at OSF: <https://osf.io/gcyqs>. Behavioural, EEG
430 and physiological raw data and main analysis code are available at:
431 https://osf.io/pqmra/?view_only=df6b8e7cd19743d481d86ef7cb83cb83. Further data and code are
432 available upon request from the first author.

433

434

435

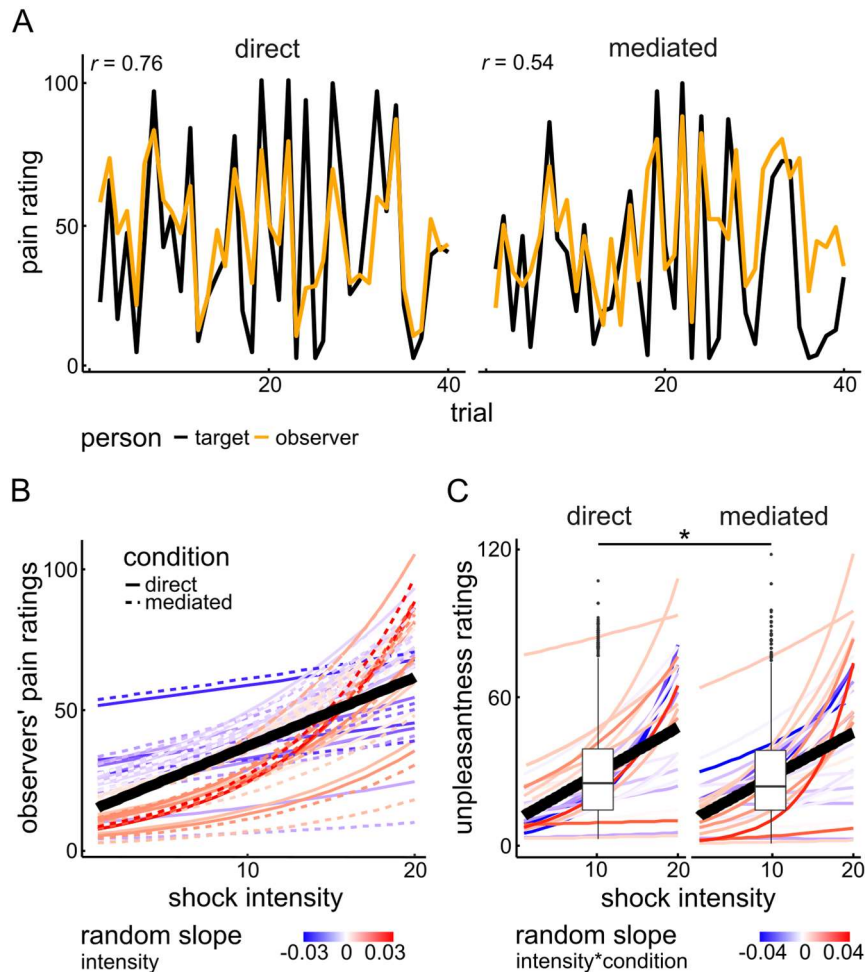
436 **Results**

437 **Empathic accuracy and unpleasantness ratings**

438 Data from 30 dyads were included in these analyses. The best generalized linear mixed model for
439 empathic accuracy had a random-effects structure containing random slopes for *condition* and *intensity*
440 (AIC difference to the next best model during fitting of random effects: -63). Moreover, it contained a
441 fixed effect of *intensity* ($b(SE) = 0.07(0.01)$, $z = 10.24$, $p < 0.0001$, AIC difference to a model without
442 the fixed effect of intensity: -14). This shows that the intensity of the shocks received by the targets
443 predicted the observers' pain ratings (Fig. 2A & B), indicating meaningful empathic accuracy. However,
444 this effect did not differ between conditions.

445 The best generalized linear mixed model for unpleasantness ratings had a random-effects
446 structure containing random slopes for the interaction between *condition* and *intensity* (AIC difference
447 to the next best model during fitting of random effects: -29). It contained a fixed effect of *intensity* ($b(SE)$
448 $= 0.07(0.01)$, $z = 8.07$, $p < 0.0001$) and a fixed effect of *condition* ($b(SE) = -0.14(0.05)$, $z = -2.63$, $p =$
449 0.009 , AIC difference to a model without the fixed effect of *condition*: -4). This shows that the intensity
450 of the shocks received by the targets predicted the observers' unpleasantness ratings (Fig. 2C), but
451 equally so in both conditions. However, the observers rated the pain of the target as slightly more
452 unpleasant in the direct than in the mediated interaction (mean difference (SD) = 1.47(6.45)).

453



454

455 **Figure 2.** (A) Example pain rating data over trials from one randomly chosen sample dyad. (B) Predicted observer
456 pain ratings for direct- and mediated-interaction conditions. The black thick line represents the fixed effect of shock
457 intensity; single coloured lines represent predicted data from single participants. The colour shading from blue to
458 red represents the value of the random slope for intensity of each participant, and the solid and dotted lines show
459 predicted ratings for direct and mediated condition, respectively. (C) Predicted observer valence ratings in direct
460 and mediated interaction. The black thick line represents the fixed effect of shock intensity; single coloured lines
461 represent predicted data from single participants. The colour shading from blue to red represents the value of the
462 random slope for the interaction between intensity and condition of each participant. The boxplots represent
463 summary statistics for each condition. * = $p < 0$.

464

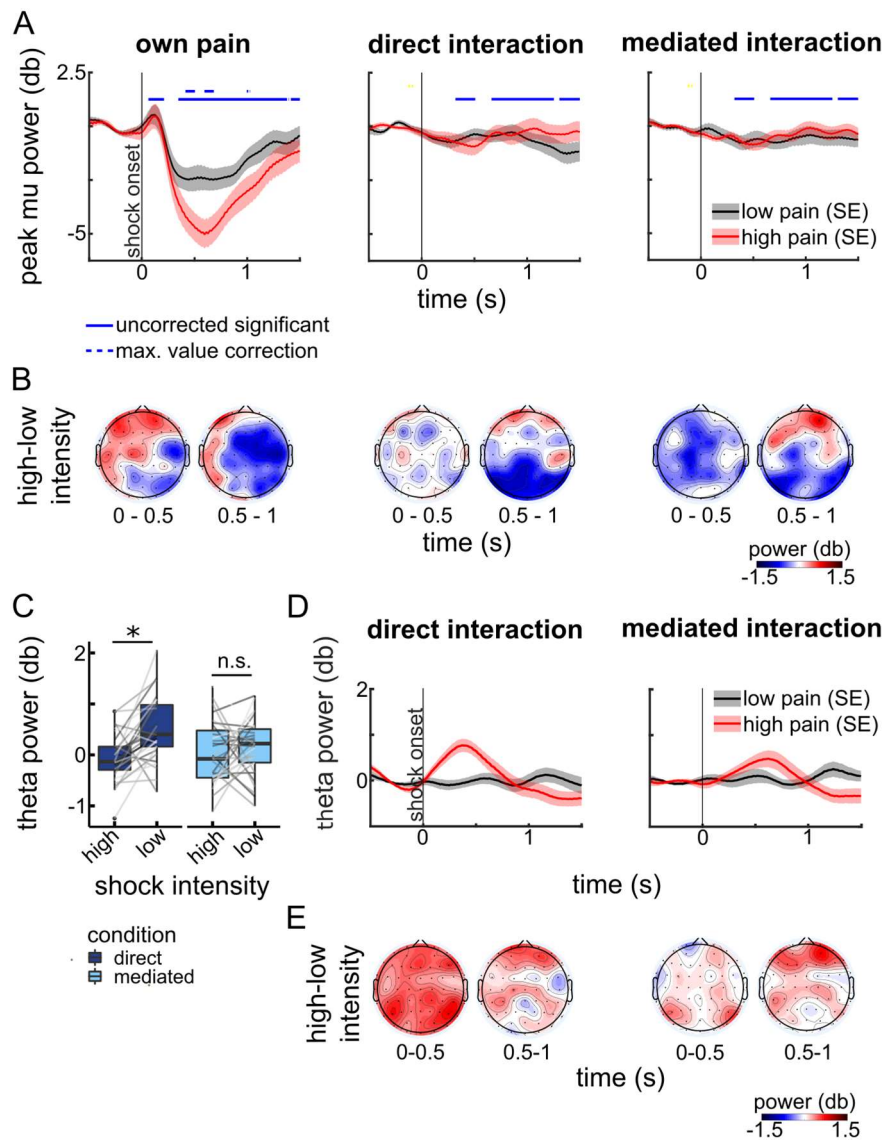
465

466 Mu suppression

467 Data from 29 dyads were included in these analyses. The analyses of peak mu suppression in the
468 “direct” and “mediated interaction” conditions showed no effect of *intensity* or *condition*, nor an
469 interaction that was significant after maximum value correction (see Fig. 3A & 3B middle and right). This
470 shows that mu suppression was not sensitive to others' pain intensity in either condition. Similarly,
471 analysing averaged power over the canonical mu band (8–13 Hz) yielded no significant effect of either
472 factor (*intensity*: $b(SE) = 0.34(0.30)$, $t(df) = 1.13(87)$, $p = 0.26$; *condition*: $b(SE) = -0.04(0.30)$, $t(df) =$
473 $-0.14(87)$, $p = 0.88$; *interaction intensity*condition*: $b(SE) = -0.02(0.42)$, $t(df) = -0.04(87)$, $p = 0.97$).

474 However, peak mu significantly differed between pain levels when participants experienced pain
475 themselves (Fig. 3A left).

476



477

478 **Figure 3.** (A) Shown is peak mu power averaged over participants, dichotomized into low- and high-intensity
479 shocks for display purposes only. Blue solid lines indicate time windows where the main effect of intensity reached
480 significance (uncorrected level); blue dotted lines indicate time windows where the intensity effect survived
481 maximum value correction. The main effect of condition and the interaction of condition x intensity did not survive
482 maximum value correction, at any time-point. On the left side, the clear effect of pain intensity on mu power in the
483 own-pain condition can be assessed. (B) Shown is the topography of averaged peak mu power differences between
484 high- and low-intensity shocks in the three conditions. (C) Shown are boxplots for theta power averaged over 4–8
485 Hz and 0–500 ms after shock onset at electrode Fz for the direct and mediated conditions. Grey lines depict means
486 from single participants. Significance asterisks refer to post-hoc tests from linear mixed models. * = $p < 0.001$. (D)
487 Shown is the time course of averaged theta power (4–8 Hz) after stimulus onset. (E) Shown is the topography of
488 averaged theta power differences between high- and low-intensity shocks in the two conditions.
489

490

491

492

493

494 **Theta band**

495 Data from 30 dyads were included in these analyses. The best-fitting linear mixed model for the power
496 averaged over the canonical theta band (4–8 Hz) yielded a significant main effect of *intensity* ($b(SE) =$
497 $0.57(0.14)$, $t(df) = 3.99(90)$, $p < 0.001$) and a significant interaction between *condition* and *intensity*
498 ($b(SE) = -0.46(0.20)$, $t(df) = -2.30(90)$, $p = 0.024$, AIC difference to next best model: 2.9). Follow-up
499 models on the interaction showed a significant effect of *intensity* in the direct condition ($b(SE) =$
500 $0.57(0.13)$, $t(df) = 4.46(28.99)$, $p < 0.001$), but not in the mediated condition ($b(SE) = 0.10(0.15)$, $t(df) =$
501 $0.70(28.99)$, $p = 0.49$). This indicated that frontal theta was more responsive to the other's shock
502 intensity in the direct condition than in the mediated condition (see Fig. 3C, D, E).

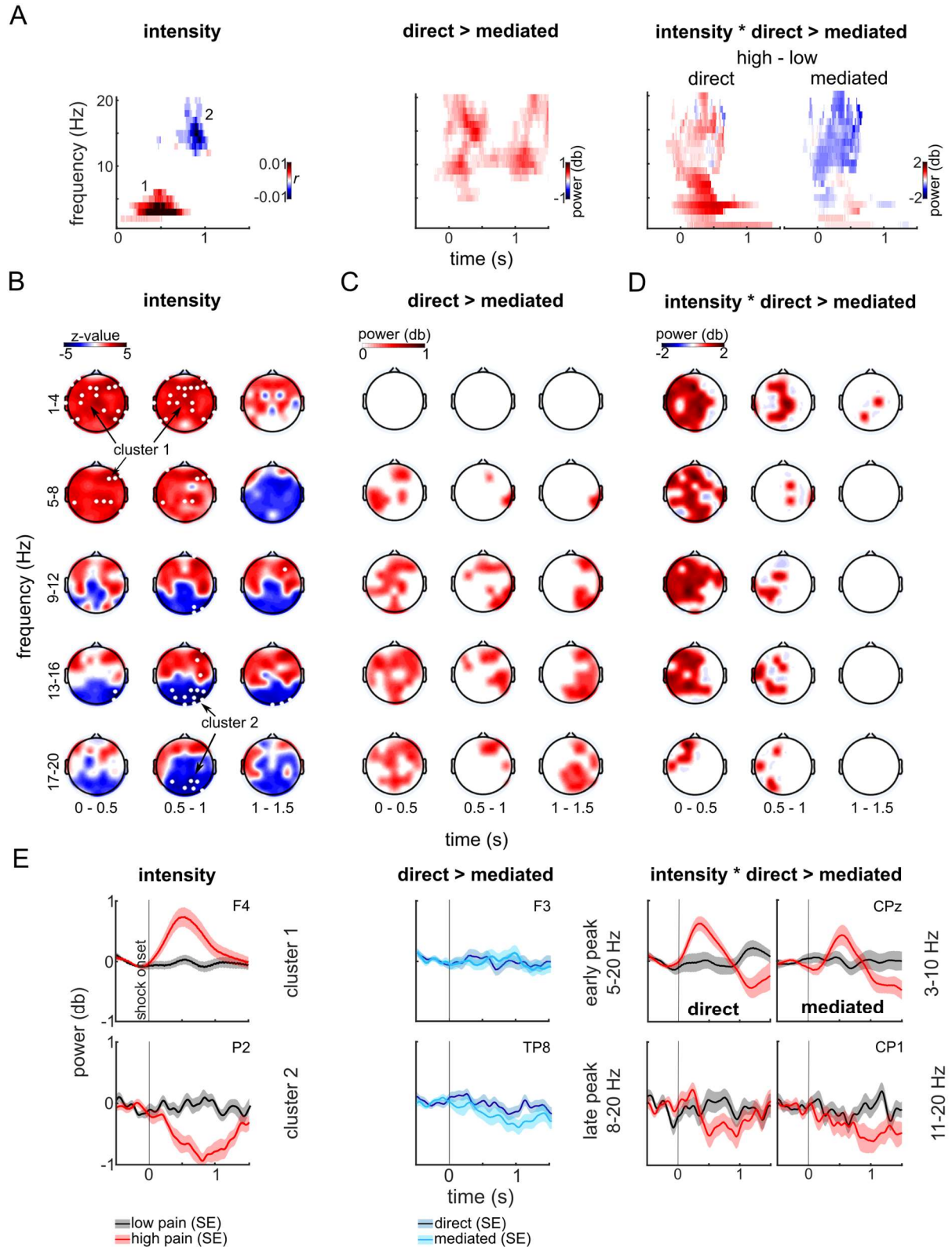
503

504 **Exploratory analyses of whole time-frequency-electrode space**

505 Data from 30 dyads were included in these analyses. During both direct and mediated interaction,
506 others' pain *intensity* was positively related to 2 to 6 Hz power between 56 and 840 ms at the frontal
507 and central electrodes (cluster 1, maximal at F4, see Fig. 4A left, B and E top left). Others' pain *intensity*
508 was also negatively related to 12- to 20-Hz power between 680 and 1040 ms over parietal and occipital
509 electrodes (cluster 2, maximal at P2, see Fig. 4A left, B and E bottom left).

510 Neither the permutation test on the *condition* effect (mediated vs. direct) nor the interaction
511 between *condition* and *intensity* yielded any cluster that survived the cluster size correction or the
512 maximum value correction. However, due to the exploratory nature of the analyses, we further
513 examined the biggest cluster, which was significant on an uncorrected level. In direct compared to
514 mediated interactions (main effect of condition; see Fig. 4A middle, C and E middle), theta/alpha (5–
515 12 Hz) power at the frontal electrodes and lower beta (13–20 Hz) power at the frontal, central and
516 centro-parietal electrodes was enhanced in an early time window (-256–644 ms). In a later time window
517 (511–1500 ms), alpha/lower beta (8–20 Hz) power at the centro-parietal electrodes was enhanced
518 during direct interactions. For the interaction between *condition* and *intensity*, the biggest uncorrected
519 significant cluster showed a stronger positive effect of *intensity* in the “direct” than in the “mediated”
520 condition. This cluster spanned 3–20 Hz between -220 and 1380 ms and included most left-hemisphere
521 and central electrodes (see Fig. 4A right, D). Its time course is displayed separately for low (3–9 Hz,

522 electrode with maximal interaction: Cz, Fig. 4E top right) and high frequencies (10–20 Hz, electrode
 523 with maximal interaction: CP1, Fig. 4E bottom right).
 524



525 **Figure 4:** (A) Clusters found in the permutation tests on the correlation between shock intensity and EEG power
 526 across both conditions (left), on the main effect of condition (middle) and on the interaction between shock intensity
 527

528 (dichotomized for display purposes only) and condition (right), averaged over electrodes. (B) Results of the
529 permutation test on the correlation between shock intensity and EEG power across direct and mediated conditions.
530 Data points that were significant after cluster size correction are displayed in colour; data points that were significant
531 after maximum value correction are marked in white. (C) Results of the permutation tests on the condition effect.
532 Data points of the largest cluster (uncorrected significant) are displayed in colour. (D) Results of the permutation
533 tests on the interaction between condition and intensity (dichotomized for display purposes only). Data points of
534 the largest cluster (uncorrected significant) are displayed in colour. (E) Power time course of cluster 1 (top left) and
535 cluster 2 (bottom left), and power time course for the early cluster (5–20 Hz, F3, middle top) and the late cluster
536 (8–20 Hz, TP8, middle bottom) showing a condition effect and power time course of lower frequencies (3–9 Hz;
537 top, right), and higher frequencies (10–20 Hz; bottom, right) for interaction effects between condition and intensity.
538 Data are dichotomized into low and high intensities for display purposes only.
539

540 **Condition effects on observers' physiological responses**

541 The best single-trial linear mixed model testing the effect of “direct” vs. “mediated” condition on
542 observers' IBI responses to the observed shocks contained random slopes for *condition* and *intensity*
543 but no fixed effects. These results indicate that observers' IBI responses were not sensitive to the
544 observed shock intensity on the sample level (see Fig. 5A).

545 Observers' SCRs were greatest in the time window from 2 to 5 seconds after shock onset,
546 hence this time window was used for all further analyses. The best single-trial linear mixed model on
547 observers' SCR to the observed shocks contained random slopes for *condition* and *intensity*, a non-
548 significant fixed effect of *condition* and a fixed positive effect of *intensity*. These results indicate that
549 observers' SCRs were sensitive to the shock intensity, but equally so in direct and mediated conditions
550 (Fig. 5C and 5D). All model parameters are listed in Table 1. Models with dichotomized intensities
551 yielded the same results.

552

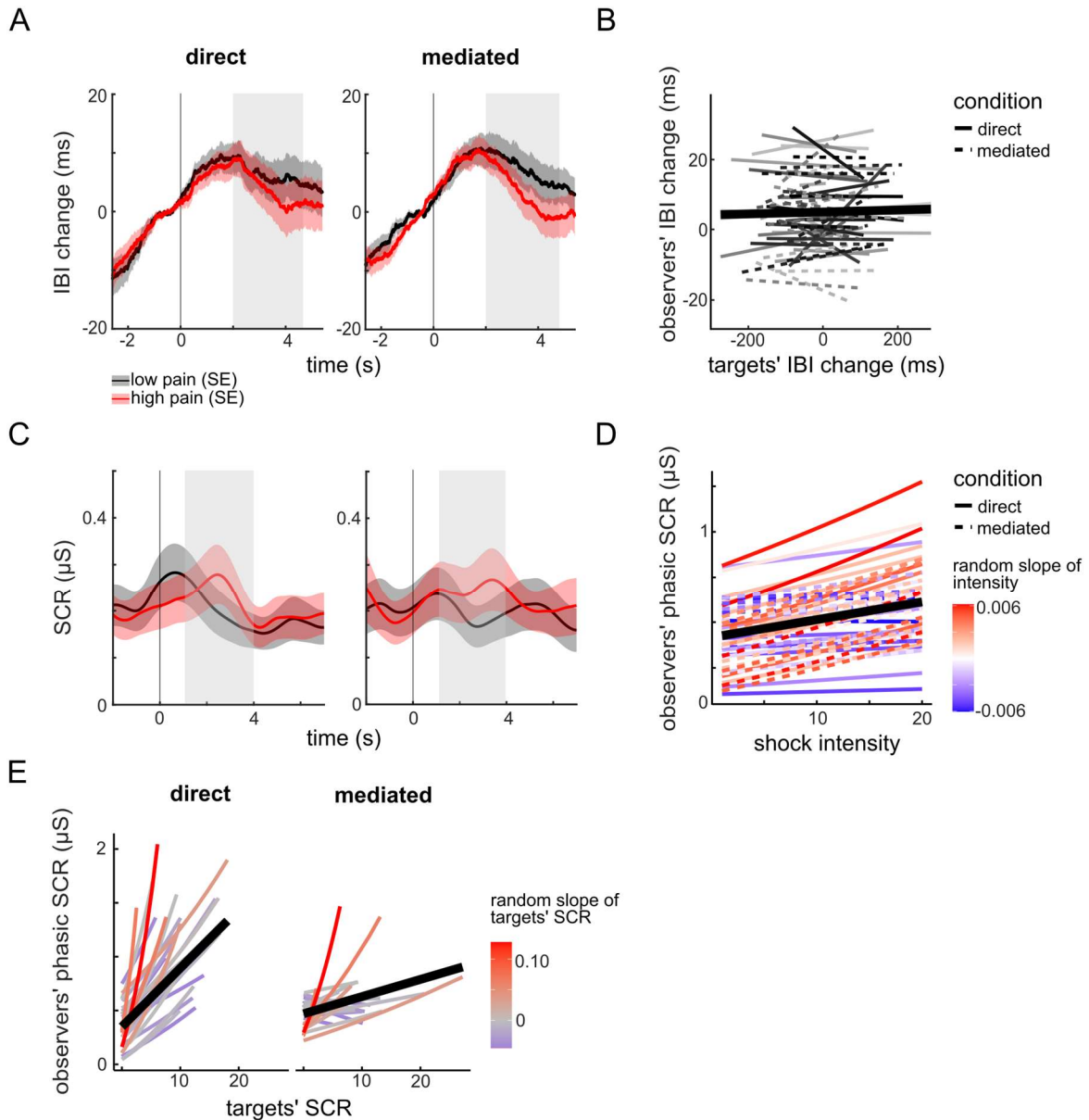
553 **Condition effects on physiological coupling**

554 The best single-trial linear mixed model testing effects of “direct” vs. “mediated” interaction on IBI
555 coupling – predicting observers' IBI responses from targets' IBI responses – contained a random slope
556 for *condition* and a fixed but not significant effect of *target IBI*. These results indicate that there was only
557 minimal coupling between targets' and observers' IBI responses, which did not differ between
558 conditions (Fig. 5B). Comparing the correlations between the continuous IBI traces in the two conditions
559 showed the same results (correlations were highest for a lag of 2 seconds).

560 The best single-trial linear mixed model on SCR coupling – predicting observers' SCR from
561 targets' SCR – contained a random slope for *condition* and *target SCR* and fixed effects of *target SCR*,
562 *condition* and their interaction (for model parameters, see Table 1). Follow-up models on the interaction
563 between *condition* and *target SCR* showed a significant positive effect of *target SCR* on observers' SCR

564 in the “direct” condition ($b(SE) = 0.12(0.03)$, $t = 4.15$, $p < 0.0001$), but not in the “mediated” condition
565 ($b(SE) = 0.03(0.02)$, $t = 1.64$, $p = 0.1$). When comparing the correlation coefficients of targets’ and
566 observers’ SCRs between conditions, there was only a marginally significant effect of *condition* ($b(SE)$
567 $= -0.07(0.04)$, $t(df) = -1.81(26)$, $p = 0.082$). These results indicate that coupling between targets’ and
568 observers’ SCRs was greater in the direct than the mediated interaction, but the effect was rather small
569 (see Fig. 5E).

570



571 **Figure 5:** (A) Grand averages of observers' IBI responses in direct and mediated interactions, dichotomized into
572 low- and high-intensity trials for display purposes only. (B) Observer IBI responses predicted from the single-trial
573 model on physiological coupling. The thick black line represents the fixed effect of target IBI; the thin lines represent
574 predicted data for single participants. (C) Grand averages of observers' SCRs in direct and mediated interactions,
575 dichotomized into low- and high-intensity trials for display purposes only. (D) Observer SCRs predicted from shock
576 intensity in the generalized linear mixed model. The black thick line represents the fixed effect of intensity; the
577

578 coloured lines display predicted values for single participants. The colour shading from blue to red represents the
579 value of the random slopes of shock intensity for each participant. Solid and dotted lines show predicted values for
580 direct and mediated conditions, respectively. (E) Observer SCRs predicted from target SCRs in the generalized
581 linear mixed model on physiological coupling. The black thick line represents the fixed effect of targets' SCRs; the
582 coloured lines display predicted values for single participants. The colour shading from blue to red represents the
583 value of the random slopes of shock intensity for each participant.
584

585 **Control analysis: Target expressivity**

586 The means of the pain ratings from the video control experiment did not differ significantly between
587 conditions (mean difference = 0.79, $t(30) = 1.66$, $p = 0.11$, Cohen's $d = 0.3$). The mean Spearman's
588 correlations between video observers' ratings and shock intensity also did not differ between videos
589 from direct and mediated interaction (mean_{direct}(SD) = 0.36(0.16), mean_{mediated}(SD) = 0.32(0.13), mean
590 difference = 0.040, $t(30) = 1.36$, $p = 0.18$). These results indicate that the targets did not express their
591 pain significantly differently in the direct versus mediated interaction.
592

593

594 **Discussion**

595 Although mediated social interactions through video calls are becoming the new norm, the impacts on
596 understanding others and their feelings have not yet been researched thoroughly (Grondin et al., 2019),
597 especially in social neuroscience. In the current study, we explored how a video-mediated interaction
598 affects empathy for pain on behavioural, physiological and neural levels. We expected that less
599 availability of social cues in a mediated interaction would hamper empathizing with the other. However,
600 we found that observers were just as accurate in judging the other's pain in the mediated interaction as
601 in the direct interaction. Moreover, participants experienced the other's suffering as only slightly less
602 unpleasant in the mediated interaction. On the neural level, mu suppression over the somatosensory
603 cortex was not sensitive to the other's pain in either condition. However, mid-frontal theta tracked the
604 other's pain intensity more in the direct than in the mediated interaction. Exploratory analyses of the
605 whole time-frequency-electrode space showed no additional differences between direct and mediated
606 conditions after correcting for multiple comparisons. On a physiological level, observers' SCRs were
607 coupled to targets' SCRs to a stronger degree in the direct compared to the mediated interaction. In
608 sum, behavioural empathy was not reduced in the mediated interaction, whereas some neural and
609 physiological aspects of empathy were dampened.

610

611 **Effects of social presence on behavioural aspects of empathy for pain**

612 Surprisingly, among the many studies on empathy for pain, hardly any measured empathic accuracy,
613 and none explored which type of information is necessary or sufficient to judge others' pain accurately
614 (Gauthier et al., 2008; Laursen et al., 2014; Leonard et al., 2013). In story-based empathy studies,
615 empathic accuracy for emotion was reduced when auditory linguistic information was completely
616 removed, whereas missing visual information did not impact empathic accuracy (Jospe et al., 2020;
617 Zaki et al., 2009a). Similarly, we reveal that participants could judge the targets' pain quite well, and
618 this ability did not decline in the mediated interaction. In contrast to the story-based paradigm, our
619 results imply that visual information (apparent in both the direct interaction and the video calls) is
620 sufficient for empathic accuracy for others' pain. As our participants did not experience severe pain
621 (expressed by moaning or crying), auditory information might have been less important than for
622 example in empathic responses to the pain of hospital patients (Agahi & Wanic, 2020). As our control
623 analysis showed no condition differences in target expressivity, we can be assured that these did not
624 mask true condition differences in empathic accuracy.

625 Although observers showed more affective empathy in the direct than in the mediated condition,
626 the effect size was so small that it was practically negligible. One reason for this might be that many of
627 our participants remembered their own recent pain experience and so were empathic to the similar
628 experience of another. This was also stated by many in the debriefing questionnaires. This strategy
629 might have led to imagination of others' pain independent of the medium, causing similar affective
630 empathy (Goubert et al., 2005).

631

632 **Effects of social presence on neural aspects of empathy for pain**

633 As most former studies on empathy for pain used abstract cues or static pictures, we expected to find
634 even stronger mu suppression in our paradigm using real stimuli and focusing on individual peak-mu
635 frequency (i.e., Perry et al., 2010a; Riečanský & Lamm, 2019; Zebarjadi et al., 2021). Instead, we did
636 not find any mu suppression in response to others' pain. Speculatively, mu suppression is a
637 compensatory mechanism that aids empathy for pain via somatosensory representation of others' pain
638 if insufficient sensory cues are available. Alternatively, it may be a weak signal that requires many
639 repetitions – and stronger pain signals – to find a significant effect. However, if mu suppression is a
640 general empathy mechanism, our analysis should have been sensitive enough to detect it. Therefore,

641 our null findings on mu suppression align with recent criticism of its robustness and validity as a
642 mechanism underlying empathy in general (Hobson & Bishop, 2016).

643 The mid-frontal theta/delta response constitutes another neural component of empathy for pain
644 that has so far been rarely examined in EEG studies (but see Mu et al., 2008; Peng et al., 2021). Mid-
645 frontal theta has been related to the salience, unexpectedness and aversiveness of many different types
646 of stimuli (Cavanagh & Shackman, 2015; González-Roldan et al., 2011; Güntekin & Başar, 2014).
647 Therefore, the heightened sensitivity of theta to the other's pain level might indicate that the other's pain
648 elicits more arousal and negative affect in the direct interaction (Balconi et al., 2009), although this did
649 not result in measurable behavioural differences. Mid-frontal theta might stem from the ACC, which
650 shows reliable activity to both own and others' pain in fMRI studies (Cavanagh & Frank, 2014; Fallon
651 et al., 2020). Confirming this assumption with source analyses was beyond the scope of this paper but
652 could be an important step in future studies. The exploratory single-trial permutation test confirmed on
653 a trend level the interaction between others' pain intensity and direct versus mediated interaction.

654 Lastly, our exploratory analysis revealed stronger parietal beta suppression relating to stronger
655 observed pain irrespective of the condition. Parietal beta decrease has been linked to attention to
656 affective touch (von Mohr et al., 2018). Future EEG studies should clarify its role in empathy for pain.

657

658 **Effects of social presence on physiological coupling**

659 Observers' cardiac activity was not sensitive to others' pain and showed no coupling with targets'
660 cardiac activity. In contrast, previous empathy studies found cardiac coupling in emotional empathy
661 (Zerwas et al., 2021), especially when semantic and auditory information was missing (Jospe et al.,
662 2020). One reason for these discrepancies might be that the shocks used in the current study elicited
663 such strong cardiac responses in targets that they were not easily mimicked by observers' cardiac
664 activity (Goldstein et al., 2017).

665 In contrast, we found coupling in skin conductance responses, and this was the one aspect of
666 pain empathy that was markedly reduced in the mediated interaction. This indicates that the
667 physiological-coupling component of empathy, specifically in SCR, might rely on physical proximity
668 (Chatel-Goldman et al., 2014; Murata et al., 2020) and possibly olfactory cues that are missing in
669 mediated interactions (Calvi et al., 2020; de Groot et al., 2014).

670

671 **Limitations**

672 The main limitation of this study is the small sample size, which was due to the complexity of the design.
673 This is especially prominent when reporting mostly null results, as one might argue that our small
674 sample size prevented us from detecting subtle effects of social presence. However, as power analyses
675 showed, by analysing single trials and using a within-subject design, we had sufficient power to detect
676 meaningful effects of social presence. Another limitation is the comparably low standardization of our
677 laboratory task. Using a task with real live people, we aimed to capture real-life empathy for pain in the
678 best way possible in the EEG laboratory. At the same time, by using a standardized pain-stimulation
679 protocol, we maintained a high degree of standardization compared to studies using unstructured
680 interactive paradigms (i.e., Levy et al., 2017). Our study therefore answers recent calls for more
681 interactive and contextual experimental methods for researching social interaction (Dumas, 2011;
682 Przyrembel et al., 2012; Sonkusare et al., 2019).

683

684 **Conclusions and future directions**

685 Many recent studies examined direct interactions between participants, claiming that this is necessary
686 for understanding social cognition (Fan et al., 2021; Levy et al., 2021; Redcay & Schilbach, 2019).
687 However, few studies have explicitly compared these new paradigms to similar tasks using mediated
688 interactions (but see e.g. Hietanen et al., 2020). Hence, it remains unclear whether the degree of social
689 presence affects social cognition and if these effects are due to the interactivity (here called
690 “immediacy”) or to the amount of information transferred and the shared physical space (called
691 “intimacy”) (Cui et al., 2013; Grondin et al., 2019). Therefore, by examining the impact of social
692 presence on empathy for the first time, we add a potentially important dimension to the study of social
693 cognition. We show that the effects are nuanced: Only the immediate mid-frontal theta response to
694 others’ pain, presumably relating to emotional arousal (Balconi et al., 2009), and SCR coupling were
695 affected by the reduced intimacy. This could indicate that intimacy is especially important for more
696 automatic, stimulus-driven empathy components. Future studies should address whether the
697 immediacy within the interaction might have a stronger impact on all components of empathy (Hamilton
698 & Lind, 2016; Hietanen et al., 2020).

699 To conclude, we do not find evidence that empathy for pain is markedly impaired in video-
700 mediated interactions, although physiological and neural resonance with the other’s pain was reduced,

701 which implies that some level of synchronization with the other is impaired. This suggests that empathic
702 abilities might be preserved in everyday mediated social interactions, which are becoming more
703 common. By showing specific changes in empathy components in a mediated interaction, we start to
704 fill the gap in knowledge about social presence in social neuroscience.

705

706

707

708

709

710

711

712 **References**

- 713 Abler, B., & Kessler, H. (2009). Emotion Regulation Questionnaire – Eine deutschsprachige Fassung
714 des ERQ von Gross und John. *Diagnostica*, 55(3), 144–152. [https://doi.org/10.1026/0012-](https://doi.org/10.1026/0012-1924.55.3.144)
715 1924.55.3.144
- 716 Agahi, S., & Wanic, R. (2020). Supremacy of auditory versus visual Input in somatic Empathy and
717 perceived Pain Level. *Pain Management Nursing: Official Journal of the American Society of*
718 *Pain Management Nurses*, 21(2), 201–206. <https://doi.org/10.1016/j.pmn.2019.06.013>
- 719 Akaike, H. (1998). Information Theory and an Extension of the Maximum Likelihood Principle. In E.
720 Parzen, K. Tanabe, & G. Kitagawa (Eds.), *Selected Papers of Hirotugu Akaike* (pp. 199–213).
721 Springer. https://doi.org/10.1007/978-1-4612-1694-0_15
- 722 Balconi, M., Brambilla, E., & Falbo, L. (2009). Appetitive vs. Defensive responses to emotional cues.
723 Autonomic measures and brain oscillation modulation. *Brain Research*, 1296, 72–84.
724 <https://doi.org/10.1016/j.brainres.2009.08.056>
- 725 Bates, D., Maechler, M., Bolker, B., Walker, S., Bojesen Christensen, R. H., Singmann, H., Da, B.,
726 Scheipl, F., Grothendieck, G., Green, P., Fox, J., Bauer, A., & Krivitsky, P. N. (2020). *Linear*
727 *Mixed-Effects Models using “Eigen” and S4* (1.1-25) [R]. <https://github.com/lme4/lme4/>
- 728 Benedek, M., & Kaernbach, C. (2010). Decomposition of skin conductance data by means of
729 nonnegative deconvolution. *Psychophysiology*, 47(4), 647–658. [https://doi.org/10.1111/j.1469-](https://doi.org/10.1111/j.1469-8986.2009.00972.x)
730 8986.2009.00972.x
- 731 Biocca, F., Harms, C., & Burgoon, J. K. (2003). Toward a More Robust Theory and Measure of Social
732 Presence: Review and Suggested Criteria. *Presence: Teleoperators and Virtual Environments*,
733 12(5), 456–480. <https://doi.org/10.1162/105474603322761270>
- 734 Bogdanova, O. V., Bogdanov, V. B., Miller, L. E., & Hadj-Bouziane, F. (2022). Simulated Proximity
735 enhances perceptual and physiological Responses to emotional facial Expressions. *Scientific*
736 *Reports*, 12, 109. <https://doi.org/10.1038/s41598-021-03587-z>
- 737 Burnham, K. P., & Anderson, D. R. (2004). Multimodel Inference: Understanding AIC and BIC in Model
738 Selection. *Sociological Methods & Research*, 33(2), 261–304.
739 <https://doi.org/10.1177/0049124104268644>

- 740 Calvi, E., Quassolo, U., Massaia, M., Scandurra, A., D’Aniello, B., & D’Amelio, P. (2020). The scent of
741 emotions: A systematic review of human intra- and interspecific chemical communication of
742 emotions. *Brain and Behavior*, *10*(5), e01585. <https://doi.org/10.1002/brb3.1585>
- 743 Cavanagh, J. F., & Frank, M. J. (2014). Frontal theta as a mechanism for cognitive control. *Trends in*
744 *Cognitive Sciences*, *18*(8), 414–421. <https://doi.org/10.1016/j.tics.2014.04.012>
- 745 Cavanagh, J. F., & Shackman, A. J. (2015). Frontal Midline Theta reflects Anxiety and cognitive Control:
746 Meta-analytic Evidence. *Journal of Physiology, Paris*, *109*(0), 3–15.
747 <https://doi.org/10.1016/j.jphysparis.2014.04.003>
- 748 Chatel-Goldman, J., Congedo, M., Jutten, C., & Schwartz, J.-L. (2014). Touch increases autonomic
749 coupling between romantic partners. *Frontiers in Behavioral Neuroscience*, *8*.
750 <https://doi.org/10.3389/fnbeh.2014.00095>
- 751 Cheng, Y., Yang, C.-Y., Lin, C.-P., Lee, P.-L., & Decety, J. (2008). The perception of pain in others
752 suppresses somatosensory oscillations: A magnetoencephalography study. *NeuroImage*,
753 *40*(4), 1833–1840. <https://doi.org/10.1016/j.neuroimage.2008.01.064>
- 754 Cohen, M. X. (2014). *Analyzing Neural Time Series Data: Theory and Practice* (1st ed.). The MIT Press.
- 755 Corcoran, A. W., Alday, P. M., Schlesewsky, M., & Bornkessel-Schlesewsky, I. (2018). Toward a
756 reliable, automated method of individual alpha frequency (IAF) quantification.
757 *Psychophysiology*, *55*(7), e13064. <https://doi.org/10.1111/psyp.13064>
- 758 Cui, G., Lockee, B., & Meng, C. (2013). Building modern online social presence: A review of social
759 presence theory and its instructional design implications for future trends. *Education and*
760 *Information Technologies*, *18*(4), 661–685. <https://doi.org/10.1007/s10639-012-9192-1>
- 761 de Groot, J. H. B., Semin, G. R., & Smeets, M. A. M. (2014). I can see, hear, and smell your fear:
762 Comparing olfactory and audiovisual media in fear communication. *Journal of Experimental*
763 *Psychology: General*, *143*(2), 825–834. <https://doi.org/10.1037/a0033731>
- 764 Decety, J., & Jackson, P. L. (2004). The Functional Architecture of Human Empathy. *Behavioral and*
765 *Cognitive Neuroscience Reviews*, *3*(2), 31. <https://doi.org/10.1177/1534582304267187>
- 766 Delorme, A., & Makeig, S. (2004). EEGLAB: An open source toolbox for analysis of single-trial EEG
767 dynamics including independent component analysis. *Journal of Neuroscience Methods*,
768 *134*(1), 9–21. <https://doi.org/10.1016/j.jneumeth.2003.10.009>

- 769 Dumas, G. (2011). Towards a two-body neuroscience. *Communicative & Integrative Biology*, 4(3), 349–
770 352. <https://doi.org/10.4161/cib.4.3.15110>
- 771 Einthoven, W., Fahr, G., & De Waart, A. (1950). On the direction and manifest size of the variations of
772 potential in the human heart and on the influence of the position of the heart on the form of the
773 electrocardiogram. *American Heart Journal*, 40(2), 163–211. [https://doi.org/10.1016/0002-
774 8703\(50\)90165-7](https://doi.org/10.1016/0002-8703(50)90165-7)
- 775 Ensenberg, N. S., Perry, A., & Aviezer, H. (2017). Are you looking at me? Mu suppression modulation
776 by facial expression direction. *Cognitive, Affective & Behavioral Neuroscience*, 17(1), 174–184.
777 <https://doi.org/10.3758/s13415-016-0470-z>
- 778 Fallon, N., Roberts, C., & Stancak, A. (2020). Shared and distinct functional networks for empathy and
779 pain processing: A systematic review and meta-analysis of fMRI studies. *Social Cognitive and
780 Affective Neuroscience*, 15(7), 709–723. <https://doi.org/10.1093/scan/nsaa090>
- 781 Fan, S., Dal Monte, O., & Chang, S. W. C. (2021). Levels of naturalism in social neuroscience research.
782 *iScience*, 24(7), 102702. <https://doi.org/10.1016/j.isci.2021.102702>
- 783 Gallo, S., Paracampo, R., Müller-Pinzler, L., Severo, M. C., Blömer, L., Fernandes-Henriques, C.,
784 Henschel, A., Lammes, B. K., Maskaljunas, T., Suttrup, J., Avenanti, A., Keysers, C., &
785 Gazzola, V. (2018). The causal role of the somatosensory cortex in prosocial behaviour. *ELife*,
786 7, e32740. <https://doi.org/10.7554/eLife.32740>
- 787 Gauthier, N., Thibault, P., & Sullivan, M. J. L. (2008). Individual and relational correlates of pain-related
788 empathic accuracy in spouses of chronic pain patients. *The Clinical Journal of Pain*, 24(8), 669–
789 677. <https://doi.org/10.1097/AJP.0b013e318173c28f>
- 790 Goldstein, P., Weissman-Fogel, I., Dumas, G., & Shamay-Tsoory, S. G. (2018). Brain-to-brain coupling
791 during handholding is associated with pain reduction. *Proceedings of the National Academy of
792 Sciences*, 115(11), E2528–E2537. <https://doi.org/10.1073/pnas.1703643115>
- 793 Goldstein, P., Weissman-Fogel, I., & Shamay-Tsoory, S. G. (2017). The role of touch in regulating inter-
794 partner physiological coupling during empathy for pain. *Scientific Reports*, 7.
795 <https://doi.org/10.1038/s41598-017-03627-7>
- 796 González-Roldan, A. M., Martínez-Jauand, M., Muñoz-García, M. A., Sitges, C., Cifre, I., & Montoya,
797 P. (2011). Temporal dissociation in the brain processing of pain and anger faces with different

- 798 intensities of emotional expression. *PAIN*, 152(4), 853–859.
799 <https://doi.org/10.1016/j.pain.2010.12.037>
- 800 Goubert, L., Craig, K. D., & Buysse, A. (2009). Perceiving Others in Pain: Experimental and Clinical
801 Evidence on the Role of Empathy. In J. Decety & W. Ickes (Eds.), *The Social Neuroscience of*
802 *Empathy* (pp. 153–166). The MIT Press.
803 <https://doi.org/10.7551/mitpress/9780262012973.003.0013>
- 804 Goubert, L., Craig, K. D., Vervoort, T., Morley, S., Sullivan, M. J. L., Williams, de C. A. C., Cano, A., &
805 Crombez, G. (2005). Facing others in pain: The effects of empathy: *Pain*, 118(3), 285–288.
806 <https://doi.org/10.1016/j.pain.2005.10.025>
- 807 Green, P., & MacLeod, C. J. (2016). SIMR: An R package for power analysis of generalized linear
808 mixed models by simulation. *Methods in Ecology and Evolution*, 7(4), 493–498.
809 <https://doi.org/10.1111/2041-210X.12504>
- 810 Grondin, F., Lomanowska, A. M., & Jackson, P. L. (2019). Empathy in computer-mediated interactions:
811 A conceptual framework for research and clinical practice. *Clinical Psychology: Science and*
812 *Practice*, 26(4), 17–17. <https://doi.org/10.1111/cpsp.12298>
- 813 Gross, J. J., & John, O. P. (2003). Individual differences in two emotion regulation processes:
814 Implications for affect, relationships, and well-being. *Journal of Personality and Social*
815 *Psychology*, 85(2), 348–362. <https://doi.org/10.1037/0022-3514.85.2.348>
- 816 Güntekin, B., & Başar, E. (2014). A review of brain oscillations in perception of faces and emotional
817 pictures. *Neuropsychologia*, 58, 33–51.
818 <https://doi.org/10.1016/j.neuropsychologia.2014.03.014>
- 819 Hamilton, A. F. de C., & Lind, F. (2016). Audience effects: What can they tell us about social
820 neuroscience, theory of mind and autism? *Culture and Brain*, 4(2), 159–177.
821 <https://doi.org/10.1007/s40167-016-0044-5>
- 822 Hess, U. (2021). Who to whom and why: The social nature of emotional mimicry. *Psychophysiology*,
823 58(1), e13675. <https://doi.org/10.1111/psyp.13675>
- 824 Hietanen, J. O., Peltola, M. J., & Hietanen, J. K. (2020). Psychophysiological responses to eye contact
825 in a live interaction and in video call. *Psychophysiology*, 57(6), e13587.
826 <https://doi.org/10.1111/psyp.13587>

- 827 Hobson, H. M., & Bishop, D. V. M. (2016). Mu suppression – A good measure of the human mirror
828 neuron system? *Cortex*, 82, 290–310. <https://doi.org/10.1016/j.cortex.2016.03.019>
- 829 Ionta, S., Costantini, M., Ferretti, A., Galati, G., Romani, G. L., & Aglioti, S. M. (2020). Visual similarity
830 and psychological closeness are neurally dissociable in the brain response to vicarious pain.
831 *Cortex; a Journal Devoted to the Study of the Nervous System and Behavior*, 133, 295–308.
832 <https://doi.org/10.1016/j.cortex.2020.09.028>
- 833 Jospe, K., Genzer, S., Klein Selle, N., Ong, D., Zaki, J., & Perry, A. (2020). The contribution of linguistic
834 and visual cues to physiological synchrony and empathic accuracy. *Cortex; a Journal Devoted*
835 *to the Study of the Nervous System and Behavior*, 132, 296–308.
836 <https://doi.org/10.1016/j.cortex.2020.09.001>
- 837 Lamm, C., Nusbaum, H. C., Meltzoff, A. N., & Decety, J. (2007). What Are You Feeling? Using
838 Functional Magnetic Resonance Imaging to Assess the Modulation of Sensory and Affective
839 Responses during Empathy for Pain. *PLoS ONE*, 2(12), e1292.
840 <https://doi.org/10.1371/journal.pone.0001292>
- 841 Laursen, H. R., Siebner, H. R., Haren, T., Madsen, K., Grønlund, R., Hulme, O., & Henningsson, S.
842 (2014). Variation in the oxytocin receptor gene is associated with behavioral and neural
843 correlates of empathic accuracy. *Frontiers in Behavioral Neuroscience*, 8.
844 <https://doi.org/10.3389/fnbeh.2014.00423>
- 845 Lawless, J. F. (1987). Negative binomial and mixed poisson regression. *Canadian Journal of Statistics*,
846 15(3), 209–225. <https://doi.org/10.2307/3314912>
- 847 Leonard, M. T., Issner, J. H., Cano, A., & Williams, A. M. (2013). Correlates of Spousal Empathic
848 Accuracy for Pain-related Thoughts and Feelings. *The Clinical Journal of Pain*, 29(4), 324–333.
849 <https://doi.org/10.1097/AJP.0b013e3182527bfd>
- 850 Levy, J., Goldstein, A., & Feldman, R. (2017). Perception of social synchrony induces mother-child
851 gamma coupling in the social brain. *Social Cognitive and Affective Neuroscience*, 12(7), 1036–
852 1046. <https://doi.org/10.1093/scan/nsx032>
- 853 Levy, J., Lankinen, K., Hakonen, M., & Feldman, R. (2021). The integration of social and neural
854 synchrony: A case for ecologically valid research using MEG neuroimaging. *Social Cognitive*
855 *and Affective Neuroscience*, 16(1–2), 143–152. <https://doi.org/10.1093/scan/nsaa061>

- 856 Lopez-Calderon, J., & Luck, S. J. (2014). ERPLAB: An open-source toolbox for the analysis of event-
857 related potentials. *Frontiers in Human Neuroscience*, 8.
858 <https://doi.org/10.3389/fnhum.2014.00213>
- 859 Misra, G., Wang, W., Archer, D. B., Roy, A., & Coombes, S. A. (2017). Automated classification of pain
860 perception using high-density electroencephalography data. *Journal of Neurophysiology*,
861 117(2), 786–795. <https://doi.org/10.1152/jn.00650.2016>
- 862 Mitchell, D. J., McNaughton, N., Flanagan, D., & Kirk, I. J. (2008). Frontal-midline theta from the
863 perspective of hippocampal “theta.” *Progress in Neurobiology*, 86(3), 156–185.
864 <https://doi.org/10.1016/j.pneurobio.2008.09.005>
- 865 Mu, Y., Fan, Y., Mao, L., & Han, S. (2008). Event-related theta and alpha oscillations mediate empathy
866 for pain. *Brain Research*, 1234, 128–136. <https://doi.org/10.1016/j.brainres.2008.07.113>
- 867 Murata, A., Nishida, H., Watanabe, K., & Kameda, T. (2020). Convergence of physiological responses
868 to pain during face-to-face interaction. *Scientific Reports*, 10(1), 450.
869 <https://doi.org/10.1038/s41598-019-57375-x>
- 870 Peled-Avron, L., Goldstein, P., Yellinek, S., Weissman-Fogel, I., & Shamay-Tsoory, S. G. (2018).
871 Empathy during consoling touch is modulated by mu-rhythm: An EEG study. *Neuropsychologia*,
872 116, 68–74. <https://doi.org/10.1016/j.neuropsychologia.2017.04.026>
- 873 Peng, W., Lou, W., Huang, X., Ye, Q., Tong, R. K.-Y., & Cui, F. (2021). Suffer together, bond together:
874 Brain-to-brain synchronization and mutual affective empathy when sharing painful experiences.
875 *NeuroImage*, 238, 118249. <https://doi.org/10.1016/j.neuroimage.2021.118249>
- 876 Perry, A., Bentin, S., Bartal, I. B.-A., Lamm, C., & Decety, J. (2010). “Feeling” the pain of those who are
877 different from us: Modulation of EEG in the mu/alpha range. *Cognitive, Affective, & Behavioral*
878 *Neuroscience*, 10(4), 493–504. <https://doi.org/10.3758/CABN.10.4.493>
- 879 Perry, A., Troje, N. F., & Bentin, S. (2010). Exploring motor system contributions to the perception of
880 social information: Evidence from EEG activity in the mu/alpha frequency range. *Social*
881 *Neuroscience*, 5(3), 272–284. <https://doi.org/10.1080/17470910903395767>
- 882 Ploner, M., Sorg, C., & Gross, J. (2017). Brain Rhythms of Pain. *Trends in Cognitive Sciences*, 21(2),
883 100–110. <https://doi.org/10.1016/j.tics.2016.12.001>
- 884 Przyrembel, M., Smallwood, J., Pauen, M., & Singer, T. (2012). Illuminating the dark matter of social
885 neuroscience: Considering the problem of social interaction from philosophical, psychological,

- 886 and neuroscientific perspectives. *Frontiers in Human Neuroscience*, 6.
887 <https://doi.org/10.3389/fnhum.2012.00190>
- 888 Redcay, E., & Schilbach, L. (2019). Using second-person neuroscience to elucidate the mechanisms
889 of social interaction. *Nature Reviews Neuroscience*, 20(8), 495–505.
890 <https://doi.org/10.1038/s41583-019-0179-4>
- 891 Reddan, M. C., Young, H., Falkner, J., López-Solà, M., & Wager, T. D. (2020). Touch and social support
892 influence interpersonal synchrony and pain. *Social Cognitive and Affective Neuroscience*.
893 <https://doi.org/10.1093/scan/nsaa048>
- 894 Riečanský, I., & Lamm, C. (2019). The Role of Sensorimotor Processes in Pain Empathy. *Brain*
895 *Topography*, 32(6), 965–976. <https://doi.org/10.1007/s10548-019-00738-4>
- 896 Rutgen, M., Seidel, E.-M., Rie ansky, I., & Lamm, C. (2015). Reduction of Empathy for Pain by Placebo
897 Analgesia Suggests Functional Equivalence of Empathy and First-Hand Emotion Experience.
898 *Journal of Neuroscience*, 35(23), 8938–8947. [https://doi.org/10.1523/JNEUROSCI.3936-](https://doi.org/10.1523/JNEUROSCI.3936-14.2015)
899 14.2015
- 900 Schiano Lomoriello, A., Meconi, F., Rinaldi, I., & Sessa, P. (2018). Out of Sight Out of Mind: Perceived
901 Physical Distance Between the Observer and Someone in Pain Shapes Observer's Neural
902 Empathic Reactions. *Frontiers in Psychology*, 9, 1824.
903 <https://doi.org/10.3389/fpsyg.2018.01824>
- 904 Shamay-Tsoory, S. G. (2011). The Neural Bases for Empathy. *The Neuroscientist*, 17(1), 7.
- 905 Short, J., Williams, E., & Christie, B. (1976). *The social psychology of telecommunications*. Wiley.
- 906 Singer, T., & Lamm, C. (2009). The Social Neuroscience of Empathy. *Annals of the New York Academy*
907 *of Sciences*, 1156(1), 81–96. <https://doi.org/10.1111/j.1749-6632.2009.04418.x>
- 908 Sonkusare, S., Breakspear, M., & Guo, C. (2019). Naturalistic Stimuli in Neuroscience: Critically
909 Acclaimed. *Trends in Cognitive Sciences*, 23(8), 699–714.
910 <https://doi.org/10.1016/j.tics.2019.05.004>
- 911 Sperl, M. F. J., Panitz, C., Hermann, C., & Mueller, E. M. (2016). A pragmatic comparison of noise burst
912 and electric shock unconditioned stimuli for fear conditioning research with many trials.
913 *Psychophysiology*, 53(9), 1352–1365. <https://doi.org/10.1111/psyp.12677>

- 914 Stropahl, M., Bauer, A.-K. R., Debener, S., & Bleichner, M. G. (2018). Source-Modeling Auditory
915 Processes of EEG Data Using EEGLAB and Brainstorm. *Frontiers in Neuroscience*, 12.
916 <https://www.frontiersin.org/article/10.3389/fnins.2018.00309>
- 917 van der Molen, M. J. W., Dekkers, L. M. S., Westenberg, P. M., van der Veen, F. M., & van der Molen,
918 M. W. (2017). Why don't you like me? Midfrontal theta power in response to unexpected peer
919 rejection feedback. *NeuroImage*, 146, 474–483.
920 <https://doi.org/10.1016/j.neuroimage.2016.08.045>
- 921 von Mohr, M., Crowley, M. J., Walthall, J., Mayes, L. C., Pelphrey, K. A., & Rutherford, H. J. V. (2018).
922 EEG captures affective touch: CT-optimal touch and neural oscillations. *Cognitive, Affective, &*
923 *Behavioral Neuroscience*, 18(1), 155–166. <https://doi.org/10.3758/s13415-017-0560-6>
- 924 Zaki, J., Bolger, N., & Ochsner, K. (2008). It Takes Two: The Interpersonal Nature of Empathic
925 Accuracy. *Psychological Science*, 19(4), 399–404. [https://doi.org/10.1111/j.1467-](https://doi.org/10.1111/j.1467-9280.2008.02099.x)
926 [9280.2008.02099.x](https://doi.org/10.1111/j.1467-9280.2008.02099.x)
- 927 Zaki, J., Bolger, N., & Ochsner, K. (2009). Unpacking the informational bases of empathic accuracy.
928 *Emotion*, 9(4), 478–487. <https://doi.org/10.1037/a0016551>
- 929 Zaki, J., Weber, J., Bolger, N., & Ochsner, K. (2009). The neural bases of empathic accuracy.
930 *Proceedings of the National Academy of Sciences*, 106(27), 11382–11387.
931 <https://doi.org/10.1073/pnas.0902666106>
- 932 Zebarjadi, N., Adler, E., Kluge, A., Jääskeläinen, I. P., Sams, M., & Levy, J. (2021). Rhythmic Neural
933 Patterns During Empathy to Vicarious Pain: Beyond the Affective-Cognitive Empathy
934 Dichotomy. *Frontiers in Human Neuroscience*, 15, 708107.
935 <https://doi.org/10.3389/fnhum.2021.708107>
- 936 Zerwas, F. K., Springstein, T., Karnilowicz, H. R., Lam, P., Butler, E. A., John, O. P., & Mauss, I. B.
937 (2021). “I feel you”: Greater linkage between friends' physiological responses and emotional
938 experience is associated with greater empathic accuracy. *Biological Psychology*, 161, 108079.
939 <https://doi.org/10.1016/j.biopsycho.2021.108079>
- 940
941
942
943
944
945
946
947

948 **Tables**

949

950 **Table 1:** Results of the single-trial (generalized) linear mixed models on IBI responses and SCRs

model	random slopes	SD	fixed effects	b(SE)	t(df)	p	AIC Δ
observers' IBI							-13
(n=29)	intercept/obs	25.01	intercept	4.33(2.16)	2.00(27.6)	0.055	
	condition/obs	13.00	-				
	intensity/obs	0.80					
	intercept/targ	7.9					
	condition/targ	0.13					
	intensity/targ	0.36					
observers' IBI (coupling with target IBI)							-50
(n=29)	intercept/obs	24.38	intercept	5.50 (2.22)	2.47 (31.7)	<0.019	
	condition/obs	12.98	target IBI	0.03(0.02)	1.66 (4312.2)	0.096	
	intercept/targ	0.000002583					
	condition/targ	0.000003744					
observers' SCR							-6
(n=27)	intercept/obs	0.16	intercept	0.35(0.04)	8.10	<0.0001	
	condition/obs	0.21	condition	-0.02(0.06)	-0.32	0.74	
	intensity/obs	0.007	intensity	0.01(0.002)	3.24	0.001	
	intercept/targ	0.03					
	condition/targ	0.03					
	intensity/targ	0.0009					
observers' SCR (coupling with target SCR)							-28
	intercept/obs	0.10	intercept	0.17(0.05)	3.34	0.0008	
	condition/obs	0.19	target SCR	0.12(0.02)	5.85	<0.0001	

Petereit et al.

Social presence and empathy

(n=27)	targ- SCR/obs	0.06	condition	0.18(0.07)	2.81	0.005
	intercept/targ	0.0000	target SCR *	-0.08(0.02)	-5.72	<0.0001
	condition/targ	0.05				
	targ SCR/targ	0.02				

951 **Notes:** IBI = interbeat interval, SCR = skin conductance response, AIC Δ = difference in Akaike
 952 information criterion to the next best model. Models on IBI responses are linear mixed models, and
 953 models on SCRs are generalized linear mixed models (note that the latter do not provide degrees of
 954 freedom for fixed effects).

955